

BEAM OPTICS MATCHING FOR INJECTOR CYCLOTRON AND COOLER SYNCHROTRON TARN-II

Shin-ichi WATANABE, Masahito TOMIZAWA, Tamaki WATANABE, Yoshitsugu ARAKAKI,
Mono YOSHIZAWA, Katsuhisa CHIDA, Takeshi KATAYAMA, Yoshinori HASHIMOTO
Tsutomu YAMAZAKI

Institute for Nuclear Study, University of Tokyo, Tokyo, Japan

Kazuhiko HOSONO, Kichiji HATANAKA
Research Center for Nuclear Physics, Osaka University, Osaka, Japan

Akira NODA, Toshiyuki SHIRAI
The Institute for Chemical Research, Kyoto University, Kyoto, Japan

Mitsutaka KANAZAWA, Koji NODA
National Institute of Radiological Sciences, Chiba, Japan

1. INTRODUCTION

A cooler-synchrotron TARN-II have been constructed in 1989 to study the accelerator physics and technology of the light and heavy ion beams. The maximum magnetic rigidity of the ring is 6.1 Tm with six-super periods of FBBDBBFO structures. A ferrite loaded RF cavity for a frequency range of 0.85 to 6.5 MHz have been installed to accelerate the beam up to 1.1 GeV for protons or 350 MeV/u for q/A of 0.5. An electron-cooling device of 100 KeV with an adiabatic expanded electron beam have been installed to study the atomic-molecular physics.

A SF-Cyclotron with K67 have been used as an injector of TARN-II. The INS SF-Cyclotron is equipped with a lot of beam lines for a variety of beam experiments with a nuclei-target and so on. A beam transport line for the TARN-II is double achromatic type because the matching free section is required. A beam analyzing magnet system have been installed to separate an injection beam with a momentum spread of 0.1 %. These constraints had become motive force to construct specific beam line with a long distance between them. There are twenty quadrupole-magnets and eight bending-magnets in the TARN-II beam transport line. A geometrical size of beam transport line is of 60 m in total length and 50.8 mm in diameter excepts the beam cross section of the ring. The slit, profile monitor and beam steering magnet have been installed to correct the center of beam axis

It is designed that transmission efficiency of the transport line is expected up to 30 % at 20 MeV proton beam [1][2]. The transported beam is injected into the ring with a multi turn injection method.

To attain those fundamental concept, present system is equipped with the following additional functions:

- (1) A visual beam adjustment (VBA) system aimed at beam envelope display assists the beam transportation batch. The VBA allow the operator to know whether the optical adjustment is set within the ideal focusing prediction or not, which is result in transmission efficiency of the beam.
- (2) The program code MAD8 gave the theoretical twiss parameter of the ring after the measurement of betatron tune values of the ring. This calculated values are moved to the MAGIC to search the matched k-values at the associated beam transport section. The calculated one is then referred in the adjustment of the Q-magnets

currents.

(3) A steering magnet system corrects the closed orbit distortion (COD) due to the alignment error of the ring. Stored current of the ring is then increased up to two or three times comparing with before the COD correction.

Further details of beam optics matching for the INS SF-Cyclotron and Cooler-Synchrotron TARN-II are presented in the following.

2. BEAM OPTICS CORRECTION OF BEAM TRANSPORT LINE

2.1. EXTRACTED BEAM ALIGNMENT

Because the ion beam extracted from INS-SF Cyclotron provides different beam axis for a variety of beam energies and nuclei's, subsequent beam steering system align those axis so as to match the center of beam transport line. A beam alignment method developed at GSI have been applied

Fig.1 shows the schematic of beam alignment at extraction point of SF-Cyclotron. This method is based on the theory which is to align the beam axis with any angle into ideal axis with the aids of beam profile monitor located at behind the Q-magnet and the two steering magnets.

The transfer matrix, position X_k and angle θ_k measured at the profile monitor is as follows:

$$\begin{bmatrix} X_k \\ \theta_k \end{bmatrix} = \begin{bmatrix} M_{11} & M_{12} \\ M_{21} & M_{22} \end{bmatrix} \begin{bmatrix} X_j \\ \theta_j \end{bmatrix}$$

If the measurement of beam profiles is carried out more than two times, the X_j and θ_j are obtained by numerically whenever no θ_k is presented. The X_j and θ_j are measured accurately by the iterative beam profile measurements and data processing using the least square method. The X_i and θ_i where the first steering magnet is presented, are obtained by the following formulae:

$$\begin{aligned} X_i &= X_j - \theta_j (L_1 + L_2) + L_1 K_2 I_2, \\ \theta_i &= \theta_j - K_1 I_1 - K_2 I_2 \end{aligned}$$

where the L_1 and L_2 are distance between the upstream steering and the downstream steering, distance between the downstream steering and the Q-magnet, respectively.

For the beam alignment, both the steering magnets are driven by the following currents:

$$\begin{aligned} I_1 &= (X_i + L_1 \theta_i) / (K_1 L_1), \\ I_2 &= X_i / (K_2 L_1). \end{aligned}$$

This current is deduced by the following boundary conditions:

$$X_j = 0,$$

$$\theta_j = 0.$$

The measurement of beam profile is carried out by the CAMAC system and microcomputer.

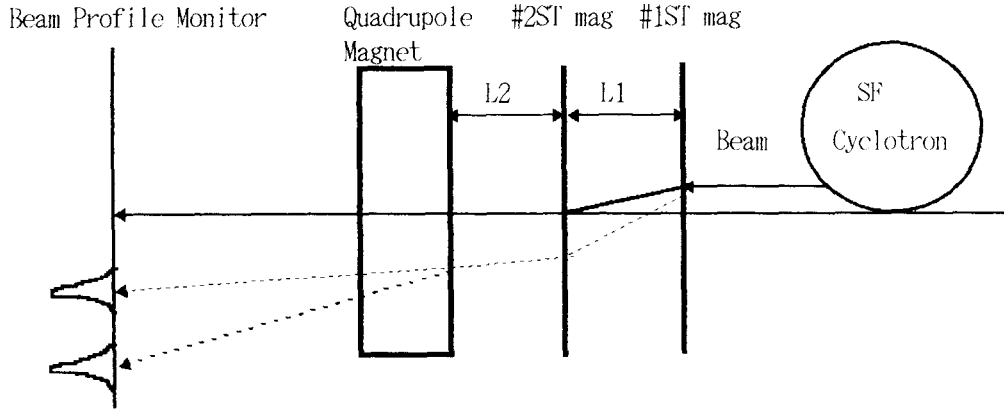


Fig.1 principal of centering of extracted beam axis

2.2. TWISS PARAMETER MATCHING

Optics mismatch becomes an origin of emittance growth in the synchrotron or storage ring. Too much emittance growth causes beam losses, which are undesirable features because they result in residual activities and short beam life. The beam size in the vertical direction has been a serious concern at the TARN-II, since large part of the beam losses occurs in the vertical direction.

The procedure of optics matching has been studied elsewhere[4]. The applied method for TARN-II is as follows (see Fig.2);

- (1) The emittances of the beam of the INS SF-Cyclotron, both in the horizontal and the vertical planes, are measured using the 1st emittance monitor (EM 1) of SF-Cyclotron transport line. The beam's twiss parameters $(\beta_{x0}, \alpha_{x0}, \beta_{y0}, \alpha_{y0})$ at an exit of SF-Cyclotron are calculated.
- (2) The emittances of the transported beam, both in the horizontal and the vertical planes, are measured using the 2nd emittance monitors (EM2) between the BT1 and the BT2.
- (3) The measured data of the phase space distributions are transferred to the position of the exit of the inflector electrode as well as exit of INS SF-Cyclotron. In this procedure, calculation is carried out by using the transfer matrix from the 2nd emittance monitor.
- (4) Using the above mentioned transferred data of the phase space distributions, the beam's twiss parameters at both places, $(\beta_x, \alpha_x, \beta_y, \alpha_y)$ at an exit of the inflector electrode and $(\beta_{x0}, \alpha_{x0}, \beta_{y0}, \alpha_{y0})$ at the exit of SF-Cyclotron are calculated by the least-squares method.
- (5) The beam's twiss parameters at the exit of inflector electrode are compared with the lattice twiss parameters of the TARN-II if the values of $\beta_{x0}, \alpha_{x0}, \beta_{y0}$ and α_{y0} coincide with the values of $\beta_{x0}, \alpha_{x0}, \beta_{y0}$ and α_{y0} .
- (6) The new k-values of quadrupole magnets between the 2nd emittance monitor and the entrance of inflector-electrode are calculated by the fitting mode of MAGIC so that the calculated twiss parameters coincide with the

Table.1 Beam parameter matching between SF Cyclotron and TARN-II

1. Beam

Initial magnetic rigidity = 1.2 Tm (Proton 66.604 MeV)

2. Initial beam parameter at the exit of Cyclotron

 $\beta_{x0}, \alpha_{x0}, \beta_{y0}, \alpha_{y0}, h_0 = 3.3226\text{m}, -1.6446\text{m}, 2.67405\text{m}, -1.64319\text{m}, 0.73\text{m}$

3. Initial beam parameter at the exit of TARN-II inflector (before the correction)

 $\beta_x, \alpha_x, \beta_y, \alpha_y = 0.6\text{m}, 0.0\text{m}, 3.27\text{m}, -0.815\text{m}$

4. Ring Twiss parameter at the exit of TARN-II inflector (injection point)

 $\beta_{xi}, \alpha_{xi}, \beta_{yi}, \alpha_{yi}, h = 10.56\text{m}, 0.210\text{m}, 5.19\text{m}, 0.519\text{m}, 4.95\text{m}$
 $\nu_x, \nu_y \text{ of the ring} = 1.7001, 1.7300$

5. Required beam parameter at the exit of TARN-II inflector (to be settled)

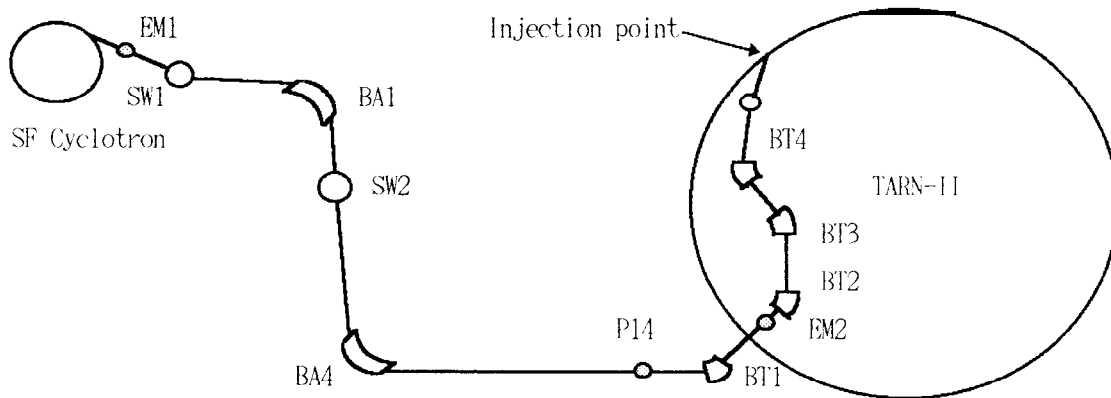
 $\beta_x, \alpha_x, \beta_y, \alpha_y, h, h' = 0.6\text{m}, 0.0\text{m}, 5.19\text{m}, 0.519\text{m}, 0.0\text{m}, 0.$

6. K-values (1/m)

Before the correction

QD6D = -1.0668128, QD6F = 1.1816571
QD5D = -1.0094891, QD5F = 0.5197765
QS = 1.1031551
QD7D = -1.3525148, QD7F = 1.2728595
QD8D = -0.909883, QD8F = 0.8165777

After 1st correction

QD6D = -1.3011370, QD6F = 1.2937391
QD5D = -0.9189236, QD5F = 0.3073576
QS = 1.3207778
QD7D = -1.3151740, QD7F = 1.3159434
QD8D = -0.7849353, QD8F = 0.8263027**Fig.2 Schematics of Twiss parameter matching**

lattice twiss parameters of TARN-II.

($\beta_x = 0.6\text{m}$, $\alpha_x = 0.0\text{m}$, $\beta_y = 5.19\text{m}$, $\alpha_y = 0.519\text{m}$ for example)

(7) The procedures (1) to (6) are repeated until matching is finished.

The result of simulation of beam optics matching is tableted in **Table.1**.

This result is obtained by the fitting mode of MAGIC. The data of ENT and VAL as the initial and final beam parameters of MAGIC are provided for examining the optics matching.

2.3. VISUAL BEAM ADJUSTMENT SYSTEM

To scope the operation of the beam handling, a model base control aiming at visual beam adjustment system (VBA) have been developed. The VBA shows the beam envelopes in x-y directions from the information of setting parameters of the beam optics. A lack of beam intensity is then estimated by this calculated beam envelopes because the VBA shows calculated envelopes together with a position scale. The VBA have been constructed based on the client-server system of TARN-II control system[5]. Two clients, for the SF cyclotron and the TARN-II, are linked with Ethernet and connected to the server machine.

At the INS SF-Cyclotron, the current data from the beam transport system are divide by the connector-box and its sub-output is fed to a CAMAC data taking system. The CAMAC data taking system in which the client-machine, send the collected data to the server-machine. Subsequently, Q-magnet current of the TARN-II area is collected by the same manner with a TARN-II data taking system. **Fig.3** shows the example of beam envelope display. The beam envelope of the transport line is calculated by the program called MAGIC or equivalent code TRANSPORT. The formulation is as follows:

$$x,y = \text{sort}(\beta_{x,y}\epsilon_{x,y}) + \eta_{x,y}(dP/P)$$

where x,y , $\beta_{x,y}$, $\epsilon_{x,y}$, $\eta_{x,y}$ and dP/P are the positions(x,y), beta functions(x,y), emittances(x,y), dispersion functions(x,y) and momentum spread, respectively.

The ratio of beam current at each stopper section and result of matrix calculation are given. To pass the cross duct with good transmission efficiency, where the beam pipe is narrowed so as to maintain a high vacuum in the ring, double achromatic designing is employed. The control of beam envelope is carried out with the Q-magnet current, but the error of beam axis ΔX_i is to be aligned by the upstream vertical or horizontal kicker magnet. For the high speed VBA, it is a best way that client executes the data collection, calculation and display of the beam envelopes simultaneously. The beam envelope is obtained by the matrix calculation.

3. BEAM DIAGNOSTIC SYSTEM

3.1 BEAM PROFILE MONITOR

The present beam profile monitors P12, P13, P14 and HM1, HM2, HM3, HM4 allow us to measure both the width and the center of beam, respectively. **Fig. 4** gave the beam profile measured at P 14. The present data shows horizontal and vertical profiles as shown in **Fig.3**. In **Fig.4** the left and right peaks show the horizontal and vertical beam profiles, respectively. Output signal from the beam profile monitor is taken by CAMAC system.

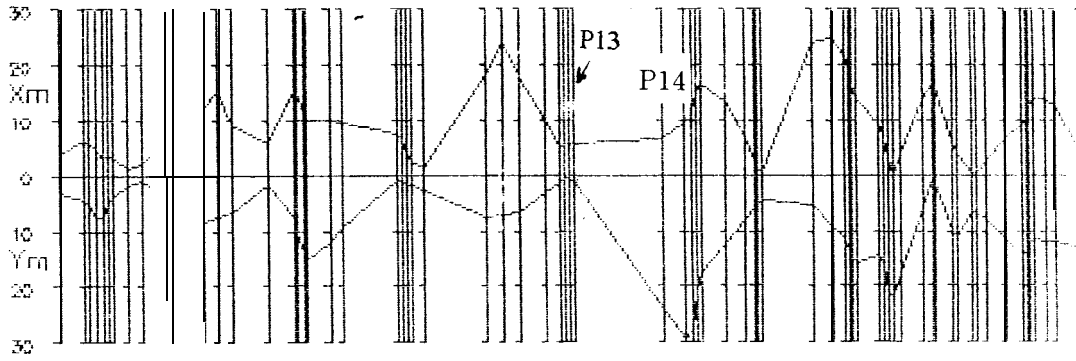


Fig.3 Calculated beam envelopes in x-y directions

The CAMAC system controls the actuator so as to move the beam detection head of profile monitor. The beam profile signal and position signal of moving head are taken by the 2 channel ADC's. The beam profile is conditioned by the noise reduction filters to reject the AC 50 Hz or higher components. Since the beam position signal is composed of 0-5 volt for horizontal and 5- 10 volt for vertical directions, data processing system identify the position, horizontal or vertical. A threshold level of beam signal have been considered to identify neither the beam signal or noise signal as shown in **Fig.4**.

3.2 BEAM EMITTANCE MONITOR

A present emittance monitor is based on the multi-drop type slit-ion collector [6]. It is convenient that horizontal and vertical emittances at an exit of SF-Cyclotron have been measured within a appropriate measuring time. The one becomes old type nevertheless superior characteristics. The emittance measurements to find the Twiss parameter of output beam from the electron linac have been studied [M.C.Ross, Y.Hashimoto[7]]. We considered to apply the same technic to measure the emittance of ion beam. It is expected that a fluorescence screen Al_2O_3+Cr for example is sensitive to the ion beam. The highly sensitivity and wide dynamic range allow us precise graphic processing with the aids of computer technology.

The basic idea behind the emittance measurements is to find the horizontal and vertical beam size ($sort(\sigma_{11})$, $sort(\sigma_{33})$) with a profile monitor as function of the strength(s) of an upstream quadrupole(s). Knowledge of the beam size at a particular location in the beam line for three different quadrupole strength is sufficient to calculate the beam sigma anywhere along the beam line. Theory of emittance measurements is as follows;

Consider a quadrupole Q of strength $k = \int B' dL / (B_0 \rho)$ separated from a down stream screen S by a transfer matrices S . The total transfer matrix of the measurement system is given by

$$R = SQ$$

where Q is the transfer matrix of the quadrupole.



Fig.4 Example of beam profile from the P14

The σ matrix is propagated through the system by the relation

$$\sigma^S = R \sigma Q R^T$$

In the absence of coupling, the square of the beam size at a given location is:

$$\sigma_{11}^S = R_{11}^2 \sigma_{11} Q + 2R_{11}R_{12} \sigma_{12} Q + R_{12}^2 \sigma_{22} Q$$

Thus by varying R (which may be done by varying one or more quadrupoles) and subsequently measuring the beam width all three elements of the sigma matrix can be obtained.

By using a thin lens approximation of above equation one sees that σ_{11}^S varies quadratically with the quadrupoles strength k :

The measured σ_{11}^S may be fit to a parabola

$$\sigma_{11}^S = A(k - B)^2 + C$$

or beam size x^2 is given by

$$x^2 = R_{12}^2 x_0^2 (k - k_0)^2 l^2 + \varepsilon^2 R_{12}^2 x_0^{-2}$$

where x_0 is the beam size at the position of the quadrupole with effective length l , k_0 is the strength of the quadrupole at the minimum beam width and R_{12} is the transfer matrix element from the end of the quadrupole to the screen. Above equation also shows that the emittance is directly related to the minimum beam size.

The above equation σ_{11}^S is obtained by the value of the σ matrix at the quadrupole, σQ ,

$$\sigma_{11} Q = A/S_{12}^2$$

$$\sigma_{22} Q = (1/S_{12}^2)(AB^2 + 2(S_{11}/S_{12})AB + (S_{11}/S_{12})^2 A + C)$$

$$\sigma_{12} Q = -(A/S_{12}^2)(B + S_{11}/S_{12})$$

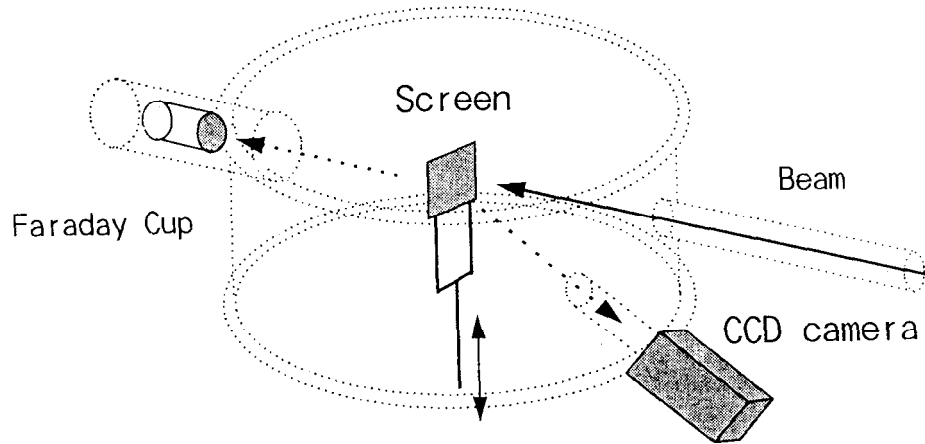


Fig.5 Schematics of beam profile measurement for Alpha 26 MeV

Fig.5 shows schematic of beam profile measurement for Alpha 26MeV extracted from INS SF-Cyclotron, The fluorescence screen $\text{Al}_2\text{O}_3+\text{Cr}$ (Demarquest AF995R) provides the highly sensitivity at a low beam current with a variety of incident beam energy. The $\text{Al}_2\text{O}_3+\text{Cr}$ plate features a heat resistance up to 1850 C and fluorescence wavelength of 700 nm [8]. It has a lifetime nearly 3 msec for average, like a ruby laser. Fluorescence due to irradiation of the beam is observed by a CCD camera providing an electric shutter. The electric shutter might be adjust both the light sensitivity and data sampling time. The background data from the CCD camera is subtracted from this measurement data so as to improve the signal-to-noise ratio. It is a record that fluorescent beam profile have been measured at an Alpha 26-MeV and 10 pA with 5 mm diameter. The dynamic range is ranging from 10 pA to 260 nA with an adjustment of the shutter speed and lens aperture of the CCD camera [9]. We have a plan to construct a new profile monitor using the new system mentioned above.

4. COD CORRJETION

The optical miss alignment of the ring districts an effective beam acceptance around a closed orbit of the ring. The main magnet was aligned within 0.3 mm at a construction phase of TARN-II. However the beam position measured by the electrostatic monitors gave the maximum COD of 20 mm. The accuracy of horizontal COD (H-COD) is expected within 1 mm at the circulating beam current of 1 μA . On the other hand, the ring gave the multi turn gain of 14 turns at the commissioning phase. Now the ring accepts the 6 turns even if we try tune the parameters no longer the COD corrections. The vertical COD (V-COD) is then estimated based on the measurement results such as a level shift and tilt of the main magnet. The program MAD gave 15 mm of the vertical COD as the maximum value[10]. It is expected that present injection gain will be improved by the correction of V-COD. The correction system is composed of the position measurement system, computer control system and correction magnet system.

The horizontal correction coil is placed at each dipole magnet around the ring. The correction of the H-COD is performed by the adjustment of local dipole field to align the center of beam orbit. To calculate the COD and perturbation field, the VAXstation 3100 is used. **Fig. 6** shows the horizontal COD before and after the corrections. In **Fig.6**, the left figure shows distorted beam position in which the bending field is set with any error comparing with an optical center field.

If the bunched beam is lost at either the left or right side of the ring, no beam position signal is observed. This constraint was examined by measuring a beam width with a beam scraper. Before the COD correction, the beam scraper gave the beam width of 70 mm at the β_x of 7 m. The measurement result shows that an effective horizontal area is more or less than 70 mm even minimum aperture of the beam monitoring devices is designed as 150 mm. The horizontal COD correction gave the resultant wide horizontal area comparing with before the correction. The vertical COD correction have been implemented by means of vertical correction magnets and electrostatic position monitor. Consequently, the injection gain have been improved from 6 to 14 turns after both the H-V COD corrections.

A transition gamma have been measured. The transition gamma deduced from the measured revolution frequency and bending magnetic field, coincides with the MAD8 within the error of 10^{-3} [11]. This result means effective length of magnetic fields gave the exact length for the calculation in the MADS.

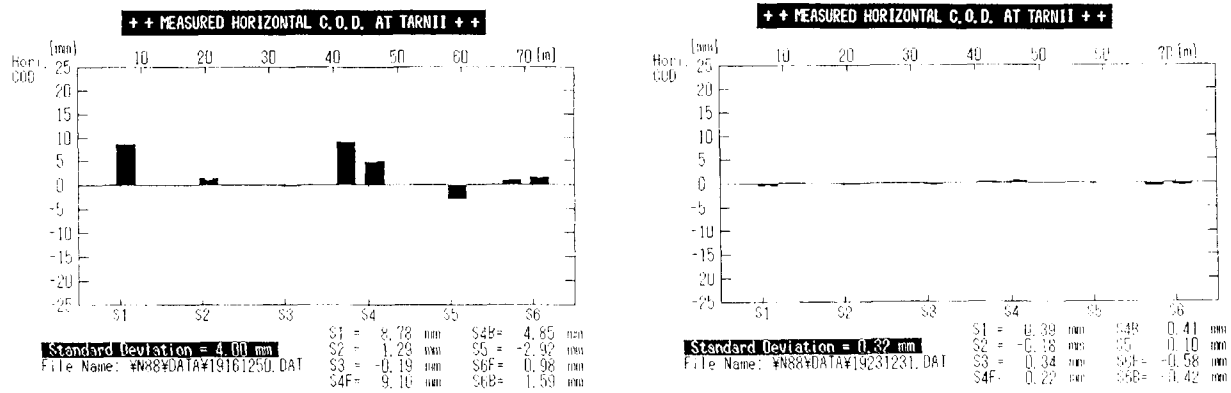


Fig.6 Measured closed orbit before and after the COD correction.

5. CONCLUSION

The optical element of the cooler-synchrotron TARN-II is set within an accuracy of several-handled micro-meter however commissioning accuracy is set within a handled micro-meter. The setting error of those optical center have been evaluated by measuring the setting errors, beam positions and beam dynamics. These errors including an elementary error of components have been compensated by using the co-operative beam correction system. Present beam correction system are exit beam centering at SF-Cyclotron, visual beam alignment system, Twiss

parameter matching and COD corrections. The measurement and adjustment of those objective have been done at a beam condition of several micro amperes. These beam optics matching result in preferable improvement of stored beam current in the ring.

REFERENCES

- [1] F.Soga *et al.* , INS-T-494, Feb. 1990
- [2] T.Hattori *et al.*, INS-NUMA-25, May 1980
- [3] T.Honma, INS-TL-146, July 1983
- [4] M.Kihara *et al.* KEK Report 93-14, Feb. 1994
- [5] S.Watanabe *et al.*, INS-Rep-1009, Nov. 1993
- [6] T.Honma, INS-TL-148, June 1985
- [7] Y.Hashimoto *et al.* INS-T-511, Aug. 1992
- [8] T.Shirai *et al.* INS-T-521, June 1993.
- [9] S.Watanabe *et al.* INS Annual report 1994.
- [10] T.Tanabe *et al.* INS Annual report 1992.
- [11] T.Watanabe *et al.* (to be published)